Interactions between Angiotensin II and NF-κB–Dependent Pathways in Modulating Macrophage Infiltration in Experimental Diabetic Nephropathy

FIONA T.H. LEE,* ZEMIN CAO,* DAVID M. LONG,*
SIANNA PANAGIOTOPOULOS,† GEORGE JERUMS,† MARK E. COOPER,* and
JOSEPHINE M. FORBES*

*Danielle Alberti Memorial Centre for Diabetes Complications, Vascular Division, Wynn Domain, Baker Medical Research Institute, Melbourne, Australia; and †Department of Endocrinology, Austin Hospital, Heidelberg, Australia

Abstract. NF-κB-dependent pathways play an important role in macrophage infiltration and kidney injury. NF-κB is regulated by angiotensin II (AII). However, the role of this pathway in diabetic nephropathy has not been clearly delineated. First, the activation of NF-κB, monocyte chemoattractant protein-1 (MCP-1), and macrophage infiltration in the diabetic kidney were explored, in a temporal manner. The active subunit of NF-κB, p65, was elevated in the diabetic animals in association with increased MCP-1 gene expression and macrophage infiltration. Second, the effects of treatment for 4 wk with the AII type 1 receptor antagonist valsartan, the AII type 2 receptor antagonist PD123319, or pyrrolidine dithiocarbamate, an inhibitor of NF-κB and on these parameters were assessed. These treatments were associated with a reduction in p65 activation, MCP-1 gene expression, and macrophage infiltration. These findings demonstrate a role for activation of NF-κB, in particular the p65 subunit, in the pathogenesis of early renal macrophage infiltration in experimental diabetes. In the context of the known proinflammatory effects of AII, it is postulated that the renoprotection conferred by angiotensin II receptor antagonism is at least partly related to the inhibition of NF-κB–dependent pathways.

NF-κB is a family of transcription factors that are usually present as dimers, the most common being the p50/p65 heterodimer (1). In contrast to the other subunits, p50 does not contain a transactivating domain. Therefore, homodimers of p50 cause gene repression rather than activation (1). NF-κB is ubiquitously expressed and is usually present in an inactive form bound to an inhibitory subunit (IκB) in the cytoplasm (1).

NF-κB has been studied extensively in renal diseases such as glomerulonephritis, tubulointerstitial disorders, and various proteinuric states (2). It is likely that NF-κB plays an important role in diabetic nephropathy as mounting evidence suggests that it is central to many interrelated pathways that contribute to the structural and functional changes of this condition (3). Some of these pathways include the renin angiotensin system (RAS), advanced glycation end product accumulation, and oxidative stress (4). In cultured endothelial cells, vascular smooth muscle cells, and proximal tubule cells, hyperglycemia itself has been shown to be able to activate NF-κB (5,6).

The renal benefits of blockade of the RAS have been well defined in experimental and human diabetes (7). Angiotensin II (AII) may contribute to renal injury in diabetes *via* its hemodynamic effects, which include an increase in intraglomerular pressure, or *via* its effects on cell proliferation and/or inflammation (8,9). There is increasing evidence to suggest a link between AII and NF-κB. NF-κB has been shown previously to be activated by AII in various *in vitro* studies, in rat mesangial (10) and mononuclear cells (11). Increased NF-κB activation was also found *in vivo* in other forms of experimental renal disease such as immune complex nephritis (11), overload proteinuria (12), and unilateral ureteral obstruction (13).

Upon activation, NF-κB is able to facilitate transcription of a number of genes, including cytokines, adhesion molecules, nitric oxide synthases, and a variety of other inflammatory and proliferative proteins involved in the pathogenesis of diabetic nephropathy (2). For example, production of the chemokine monocyte chemoattractant protein-1 (MCP-1) by mesangial cells has been postulated to be part of an early inflammatory process that causes renal injury in diabetes (14). Transcription of MCP-1 is primarily regulated by NF-κB in endothelial (15), smooth muscle (16), proximal tubular (17), and mesangial cells (18,19).

Therefore, the aims of the present study were, first, to explore the temporal activation of NF-κB, particularly its major subunits p50 and p65, in diabetic kidney. In addition, the NF-κB–dependent chemokine MCP-1 and a functional manifestation of this chemokine, macrophage infiltration, were also

evaluated (protocol 1). On the basis of the findings for this first protocol, in a separate experiment, the effects of AII receptor antagonism, with AII type 1 receptor (AT1) or AII type 2 receptor (AT2) antagonists, and NF-κB inhibition, with pyrrolidine dithiocarbamate (PDTC), were evaluated in diabetic rats (protocol 2).

Materials and Methods
Experimental Model
Protocol 1. Streptozocin in citrate buffer (55 mg/kg) was injected intravenously after an overnight fast into Male Sprague Dawley rats (Animal Resource Centre, Perth, Western Australia, Australia) to induce experimental diabetes. Animals with plasma glucose concentration >15 mmol/L 1 wk after injection of streptozocin were included in the study as diabetic. Sham-injected control animals (sodium citrate buffer pH 4.5 alone) were followed concurrently. Long-acting insulin (ultratard HM; Novo Industries, Bagsvaerd, Denmark) was administered to the diabetic animals at a dose of 2 U/d by subcutaneous injection to improve the well-being of the animals, to promote weight gain, and to avoid ketonuria. The animals had unrestricted access to water and standard rat diet. The animals were killed by decapitation after 4 ($n = 8$), 12 ($n = 6$), 20 ($n = 8$), or 32 ($n = 8$) wk of diabetes. Kidneys were removed and either snap-frozen in liquid nitrogen and stored at $-70°C$ or fixed in formalin and paraffin embedded for subsequent immunohistochemistry. All animal procedures were in accordance with guidelines set by the Austin and Repatriation Medical Centre Animal Ethics Committee and the National Health and Medical Research Council of Australia.

Protocol 2. Experimental diabetes was induced in male Sprague Dawley rats as outlined above. The diabetic animals were divided into four groups ($n = 8$ in each group). The first group received no treatment, the second group received the AT1 receptor antagonist valsartan (30 mg/kg by gavage), the third group received the AT2 receptor antagonist PD123319 (5 mg/kg per day *via* Alzet osmotic pumps (model 2ML4; Alza Corporation, Palo Alto, CA), and the fourth group received the NF-κB inhibitor PDTC (5 mg/kg per day *via* osmotic pumps). The osmotic pumps were inserted subcutaneously in the midscapular region, 2 d after induction of diabetes. The doses of valsartan and PD 123319 used in this study have been previously shown to cause blockade of AT1 and AT2 receptors in the kidney (20). The dose of PDTC was adjusted on the basis of previous studies that had used noncontinuous intraperitoneal injections (21). We confirmed in pilot studies that this dose administered *via* an Alzet osmotic pump was associated with reduction in NF-κB activation. All diabetic animals received no insulin but had unrestricted access to water and standard rat diet. The animals were killed by decapitation after 4 wk of diabetes. The kidneys were removed and processed as in protocol 1.

Functional Measurements
Every 4 wk, body weight was measured and blood was collected from the tail vein for measurement of glycated hemoglobin (GHb) by HPLC (22). Animals were placed in metabolic cages for 24 h to collect urine. Urinary albumin concentration was determined by RIA as previously reported (23). Urinary albumin excretion was then subsequently calculated after correcting for urine volume (mg/24 h). Systolic BP was measured by indirect tail-cuff plethysmography in prewarmed, unanesthetized animals (24). Systolic BP was calculated as the mean value of three measurements.

Histologic Assessment of Kidney Injury
The degree of glomerulosclerosis was evaluated by a semiquantitative method as described previously. In brief, 2-μm kidney sections were stained with periodic acid-Schiff and observed under a light microscope in a masked manner at a magnification of $\times400$ using the Analysis Imaging System (AIS; Imaging Research, St. Catherines, Ontario, Canada). Forty glomeruli in each kidney were graded according to the severity of the glomerular damage: 0, normal; 1, slight glomerular damage, the mesangial matrix and/or hyalinosis with focal adhesion, involving <25% of the glomerulus; 2, sclerosis of 26 to 50%; 3, sclerosis of 51 to 75%; 4, sclerosis of >75% of the glomerulus. The indices for glomerulosclerosis were calculated using the formula $GS = (1 \times n_1) + (2 \times n_2) + (3 \times n_3) + (4 \times n_4)/n_0 + n_1 + n_2 + n_3 + n_4$, where n_x is number of glomeruli in each grade of glomerulosclerosis. The coefficient of variation in this method was 1.7%.

The evaluation of tubulointerstitial area (TIA) was assessed using a point-counting technique and performed in the renal cortex for each animal following routine established methods. In each field, 100 points were counted on a 1-cm^2 eyepiece graticule with 10 equidistant grid lines. A total of 12 high-power fields ($\times400$) per section were counted for each animal in all groups in the corticomedullary field. Each high-power field was 0.076 mm^2 with 0.91 mm^2 being the total area counted per slide.

% Fractional area (FA) was calculated as follows:

$$\% \ FA = \frac{\text{number of tubulointerstitial grid intersections}}{\text{total number of grid intersections}} \times 100$$

where %FA corresponds to the percentage of tubulointerstitial area in the total area counted of the section.

Extraction of Nuclear Proteins
As described previously (25), ~100 mg of frozen kidney cortex was weighed and homogenized. Detergent (IGEPAL CA- 630; Sigma chemical Co., St. Louis, MO) was then added to the homogenate to a final concentration of 0.7% and the homogenate was processed by further centrifugation and resuspension in buffers A and B. The supernatant was removed and frozen in aliquots at $-70°C$. Protein content was determined using the bicinchoninic acid method (Pierce Pharmaceuticals, Rockford, IL) (26).

Electromobility Shift Assay
As described previously (25), double-stranded NF-κB consensus oligonucleotides (5'-AGTTGAGGGGACTTTC-

CCAGG-3'; Promega, Madison, WI) were end labeled with γ32P-dATP (GeneWorks Pty Ltd, Adelaide, SA, Australia) using T4 kinase (Promega) and T4 kinase buffer (Promega). Binding of nuclear protein to radiolabeled oligonucleotide was performed by equilibrating nuclear extract in a mixture that contained 7 μg of nuclear protein extract, 0.25 μl of poly dI.dC (Amersham Pharmacia Biotech, Buckingham-shire, UK), and 10 μl of binding buffer (5 mM MgCl$_2$, 5 mM Tris-HCl, 20% glycerol, 2.5 mM EDTA, 2.5 mM dithiothreitol). After this, 1 μl of ^{32}P-labeled NF-κB probe (150,000 cpm, Cherenkov counting) was added. The DNA-protein complexes were resolved by nondenaturing 7% PAGE (Tris, borate, EDTA). The gel was run at 150 V for 50 min. Autoradiographs were prepared by exposing the dried gel to x-ray film (Kodak Biomax, Integrated Sciences, Melbourne, Australia) with intensifying screens for 7 to 12 h at −70°C.

The specificity of the NF-κB electromobility shift assay (EMSA) was determined with reactions that contained 100-fold excess of either unlabeled NF-κB oligonucleotide or mutant NF-κB oligonucleotide (5'-AGTTGAGGCGACTTTC-CCAGG-3'; Santa Cruz Biotechnology, Santa Cruz, CA). To determine the subunit composition of the NF-κB complexes, we performed supershift analysis using antibodies to either the p50 subunit (Santa Cruz Biotechnology) or the p65 subunit (Chemicon International, Temecula, CA). EMSA supershift was performed on six samples from each group.

Immunohistochemistry for the p50 Subunit of NF-κB, ED-1, and IκBα

Immunohistochemical studies were performed on formalin-fixed, paraffin-embedded kidney sections (4 μm) that were dewaxed and hydrated as described previously (25). Antigen retrieval for monocytes/macrophages (ED-1) immunohisto-chemistry was completed with protease digestion (0.0125 g of bacterial protease VIII [Sigma Chemical] in 50 ml of PBS for 3 min at 37°C). Antigen retrieval for IκBα was performed with 0.05 g of trypsin and 0.05 g of calcium chloride in 50 ml of TBS for 25 min at 37°C. Antigen retrieval for the activated p65 subunit of NF-κB (nuclear localization sequence) was per-formed by microwaving in 0.01 M citrate buffer (pH 6.0) for 2 × 10 min. The protein expression of activated p50 subunit of NF-κB (NLS region) was assessed using the DAKO Catalyzed Signal Amplification System (DAKO Corporation, Carpinte-ria, CA). A modification of the ABC Ig enzyme technique was used, as described previously (25), for ED-1 and IκBα. Pri-mary antibodies included rabbit anti-p50 (0.5 μg/ml; Santa Cruz Biotechnology) diluted 1:500 in TBST and applied for 15 min, mouse anti-rat ED-1 antibody (Serotec, Oxford, UK; 0.25 mg/0.25 ml) diluted 1:50 in 10% horse serum applied for 1 h at room temperature, mouse anti-p65 (0.2 μg/ml; Chemicon International) applied in 1% BSA overnight at 4°C, and rabbit polyclonal IκBα (Santa Cruz Biotechnology) diluted 1:100 in PBS applied overnight at 4°C. Tissue sections were then stained with biotinylated IgG (Vector Laboratories, Burlin-game, CA). Avidin biotin complex (Vectastain ABC Elite Kit; Vector Laboratories) was applied for 30 min. Sections were

developed for 4 min using 3,3'-diaminobenzidine in 0.1 mol/L PBS containing 0.03% hydrogen peroxide. The slides were then counterstained with Harris hematoxylin, dehydrated, mounted, and coverslipped using dePex (BDH). Negative con-trols were prepared by replacing the primary antibody with PBS. These negative controls showed no immunoreactivity (data not shown).

Quantification of p50 and IκBα staining in the kidney cortex was performed using a videoimaging system (Video Pro 32; Leading Edge, Bedford Park, SA, Australia) connected to a Zeiss AXIO-PHOT microscope (Stuttgart, Germany) (27). Measurements were performed in a masked manner by a single observer. In 15 to 20 high-power fields (×400) per section, the number of ED-1–positive cells within a 1-cm^2 eyepiece grati-cule with 10 equidistant grid lines was counted. The result was expressed as the average number of ED-1–positive cells per area counted (×400).

Determination of mRNA Levels of MCP-1

Six micrograms of total RNA extracted from each kidney was used to synthesize cDNA with the Superscript First Strand synthesis system for reverse transcription–PCR (RT-PCR; Life Technologies BRL, Grand Island, NY). Gene expression was analyzed by real-time quantitative RT-PCR performed with the TaqMan system based on real-time detection of accumulated fluorescence (ABI Prism 7700, Perkin-Elmer, Foster City, CA) (28). Fluorescence for each cycle was analyzed quantitatively by an ABI Prism 7700 Sequence Detection System (Perkin-Elmer, PE Biosystems, Foster City, CA). For controlling for variation in the amount of DNA available for PCR in the different samples, gene expression of the target sequence was normalized in relation to the expression of an endogenous control, 18S ribosomal RNA (rRNA; 18S rRNA TaqMan Control Reagent kit; ABI Prism 7700). Primers and TaqMan probe for MCP-1 (forward primer, CTCAGCCAGATGCAGTTAATGC; reverse primer, AGC-CGACTCATTGGGATCAT; probe, 6FAM-CACCTGCTGC-TACTCATTCACTGGCAA-TAMRA) and the endogenous ref-erence 18S rRNA were constructed with the help of Primer Express (ABI Prism 7700). The amplification was performed with the following time course: 50°C for 2 min and 95°C for 10 min and 40 cycles at 94°C for 20 s and at 60°C for 1 min. Each sample was tested in triplicate. Results are expressed relative to control kidney values, which were arbitrarily assigned a value of 1.

Statistical Analyses

Results are expressed as mean ± SEM unless otherwise specified. Analyses were performed by ANOVA followed by *post hoc* analysis using Fisher least significant difference method, correcting for multiple comparisons. $P < 0.05$ was considered to be statistically significant.

Results
Protocol 1

Biochemical and Metabolic Parameters. At all four time points, diabetic rats had significantly elevated GHb and plasma glucose levels and lower body weight as compared with control rats (Table 1). Despite this, the diabetic animals had larger

Table 1. Metabolic parameters in protocol 1: Time course of NF-κB activation[a]

Group	n	Glucose (mmol/L)	GHb (%)	Body Weight (g)	Kidney Weight (g)	Urine Volume (ml/24 h)	Albumin Excretion Rate[b] (mg/24 h)	Glomerulosclerotic Index	Tubulointerstitial Area (%)
4 wk C	8	6.9 ± 0.2	4.1 ± 0.2	370 ± 20	1.48 ± 0.02	14 ± 6	0.28 ×/÷ 1.3	1.3 ± 0.3	2.2 ± 0.1
4 wk D	8	31.0 ± 1.7[c]	13.8 ± 0.3[c]	315 ± 28[d]	1.76 ± 0.04[e]	136 ± 35[c]	0.47 ×/÷ 1.2	1.2 ± 0.3	3.0 ± 0.2[d]
12 wk C	6	5.4 ± 0.2	3.6 ± 0.2	453 ± 8	1.44 ± 0.04	15 ± 1	0.46 ×/÷ 1.2	1.2 ± 0.1	2.2 ± 0.1
12 wk D	6	22.1 ± 1.7[c]	10.6 ± 0.4[c]	302 ± 15[c]	1.61 ± 0.08	121 ± 12[c]	1.04 ×/÷ 1.2[d]	1.1 ± 0.3	2.8 ± 0.4[d]
20 wk C	8	7.4 ± 0.2	3.2 ± 0.1	684 ± 16	1.91 ± 0.06	18 ± 3	0.95 ×/÷ 1.2	0.9 ± 0.4	1.8 ± 0.2
20 wk D	8	27.4 ± 0.9[c]	14.2 ± 0.4[c]	390 ± 31[c]	2.34 ± 0.19[d]	130 ± 39[c]	5.01 ×/÷ 1.3[e]	0.9 ± 0.3	3.0 ± 0.4[d]
32 wk C	8	6.4 ± 0.2	4.6 ± 0.3	686 ± 18	1.49 ± 0.18	20 ± 2	4.18 ×/÷ 1.4	1.4 ± 0.2	1.9 ± 0.3
32 wk D	8	24.1 ± 2.6[c]	14.7 ± 0.9[c]	536 ± 18[c]	2.37 ± 0.24[d]	140 ± 37[e]	42.07 ×/÷ 1.4[e]	2.7 ± 0.3[d,f]	7.6 ± 0.1[c,f]

[a] Data are shown as mean ± SEM. Body weight and urine volume are expressed as mean ± SD. AER, albumin excretion rate; C, control; D, diabetic.
[b] Shown as geometric mean ×/÷ tolerance factor.
[c] $P < 0.0001$, [d] $P < 0.05$, [e] $P < 0.01$ versus respective control; [f] $P < 0.001$ versus 4, 12, and 20 wk D.

kidneys ($P < 0.01$ at 4 wk, $P = 0.11$ at 12 wk, $P < 0.05$ at 20 and 32 wk). Urine volume was significantly increased with diabetes at all time points. Albumin excretion rate was significantly elevated from week 12 onward ($P < 0.05$ at 12 wk, $P < 0.01$ at 20 and 32 wk).

Structural Parameters. Diabetes-associated increases in the glomerulosclerotic index (GSI) were seen only at week 32 (Table 1). There were no differences in GSI between control and diabetic kidneys at any other time point. Tubulointerstitial area was significantly increased in diabetic animals by week 4 and increased further at each time point as compared with controls, being maximal at week 32 (Table 1).

EMSA. EMSA on nuclear extracts from kidney cortex showed evidence of two bands. With the addition of 100-fold excess concentration of competitive cold oligonucleotide, there was elimination of both bands, indicating specificity for NF-κB. However, addition of mutant NF-κB oligonucleotide resulted in the loss of the lower band, suggesting specific NF-κB binding only in the upper band as previously reported (1).

EMSA was performed on six to eight animals at each time point. The resulting band density of diabetic and control animals was then compared and expressed as a percentage of an external control sample run on each individual gel. At 4 and 20 wk, there was no significant change in total active NF-κB (Figure 1). There was a threefold increase in NF-κB after 12 wk of diabetes. By 32 wk, however, there was a significant decrease in this parameter with diabetes.

By supershift analysis, in control animals, p50 was the main subunit contributing to total NF-κB band density (Figure 1). In diabetic animals, although p50 remained the major subunit, the percentage contribution by p65 was increased at all time points compared with controls (Figure 2A). This increase in p65 with diabetic animals was greatest at 4 wk with a reduction over time. In contrast, the changes in p50 in diabetic animals paralleled those seen with total activated NF-κB.

Activated p50 Subunit of NF-κB. Immunohistochemistry demonstrated evidence of the activated p50 subunit of NF-κB throughout the kidney, particularly in proximal and distal tubular cells (Figure 3). There was occasional staining of glomerular cells. The proportional area stained was significantly increased in diabetes at 12 wk and was significantly reduced in diabetic animals at 32 wk (Figure 4A). There was no significant change in proportional area of p50 staining with diabetes at 4 or 20 wk. There was no staining seen in the negative control sections (Figure 3E). Staining for activated p50 paralleled changes in total NF-κB activation as detected by EMSA (Figure 1A) and activated p50 (Figure 1B) as assessed by the supershift assay.

IκBα Immunohistochemistry. When compared with control animals, there was a significant increase in IκBα with diabetic kidney only at 12 wk (Figure 4B). At all other time points, there were decreases in IκBα. Overall, the diabetes-induced change in IκBα reflected changes in activated NF-κB as detected by EMSA (Figure 1A) and immunohistochemistry for the activated p50 subunit (Figure 4A).

MCP-1 Gene Expression. MCP-1 gene expression was increased by 4 wk in diabetic kidneys (Figure 2B). At 12 wk,
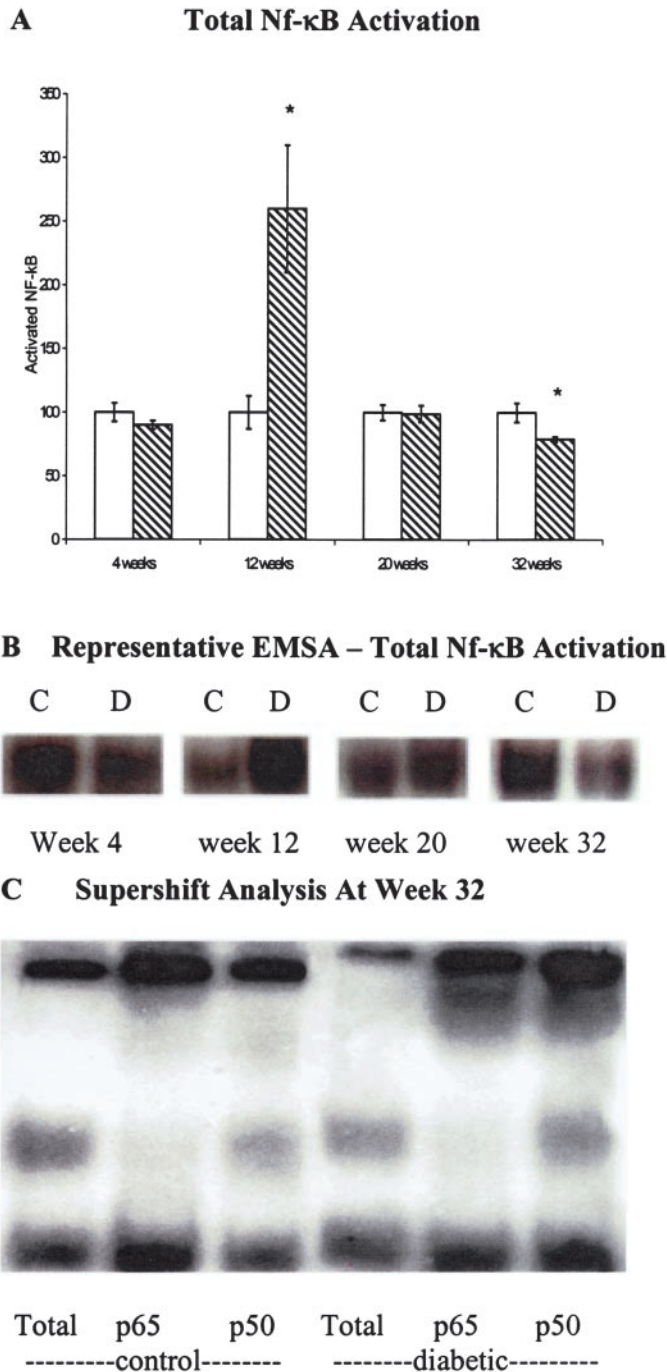
A   Total Nf-κB Activation

B   Representative EMSA – Total Nf-κB Activation

C   D   C   D   C   D   C   D

Week 4   week 12   week 20   week 32

C   Supershift Analysis At Week 32

Total   p65   p50   Total   p65   p50
---------control--------   --------diabetic---------

Figure 1. (A) Quantification of the time course of total renal activated NF-κB by electromobility shift assay (EMSA). □, controls; ▨, diabetic by striped bars. Densities of NF-κB band in diabetic group were expressed as percentage change compared with control at the same time point. *$P < 0.05$ *versus* control. (B) Representative renal EMSA acrylamide gel demonstrating total NF-κB at each time point. (C) Representative EMSA supershift gel (C) in control and diabetic rats at week 32 (1 and 3, no addition of antibody; 2 and 4, addition of antibody to p65 subunit; 3 and 6, addition of antibody to p50 subunit).

there was only a small increase in MCP-1 expression with diabetes, but this was followed by a significant decrease by 20 and 32 wk. The changes in renal gene expression for MCP-1 between diabetes and control animals paralleled changes seen with respect to the p65 subunit (Figure 2A).

ED-1 Immunohistochemistry. The number of monocytes/macrophages expressed as ED-1–positive cells per area counted was elevated in diabetic animals at all time points (Figures 2C and 5). This difference was greatest at 4 wk and decreased over time. The temporal changes in renal macrophage infiltration in the diabetic kidney paralleled the changes in MCP-1 gene expression (Figure 2B) and assessment of p65 by supershift analysis (Figure 2A).

Protocol 2

Biochemical and Metabolic Parameters. After 4 wk of diabetes, plasma glucose was significantly elevated compared with control animals (Table 2). BP was significantly elevated in diabetic animals and was significantly reduced by treatments except insulin. Diabetic animals had significantly lower body weight than control animals, but kidney weight was elevated in diabetic rats. Valsartan and PDTC, however, were associated with significantly lower kidney weights than seen in untreated diabetic rats. Albumin excretion rate was mildly increased in diabetic rats. Treatment of diabetic animals with valsartan was associated with a significant reduction in albuminuria as compared with untreated animals.

Structural Parameters. There was no increase in GSI seen with diabetes by week 4. However, treatment with valsartan produced a significant decrease, albeit modest in GSI (Table 2). Diabetes induced a significant increase in tubulointerstitial area by week 4. This increase was attenuated by treatment with either valsartan or the NF-κB inhibitor PDTC. No beneficial effects on tubulointerstitial area were noted for PD123319 (Table 2)

EMSA and Supershift Assay. At 4 wk, only PDTC caused a significant reduction in activated total NF-κB in the diabetic rats. Supershift assay showed that p50 accounted for the majority of the NF-κB band in all groups. However, the p65 subunit was elevated in diabetic animals and was attenuated by valsartan, PD123319, and PDTC treatment (Figure 6A).

Immunohistochemistry for p65 and p50 Subunits. Immunohistochemistry for p50 paralleled changes in total activated NF-κB as detected by EMSA (Figure 7B). There was a reduction with diabetes that was not significantly affected by valsartan or PD123319 treatment. PDTC reduced activated p50 to a level below all other groups. Consistent with the EMSA findings, immunohistochemistry for the activated p65 subunit of NF-κB was increased by diabetes at 4 wk. Localization of p65 was demonstrated within nuclei of both tubular epithelial cells and glomerular cells, which was minimal in control tissues (Figure 8). There was some reduction in the distribution and intensity of staining seen within treatment groups at 4 wk.

MCP-1 Gene Expression. Real-time RT-PCR revealed in diabetic animals a significant increase in MCP-1 gene expression that was significantly reduced by valsartan and PDTC, with a more modest reduction with PD123319 treatment (Figure 6B). These changes in MCP-1 gene expression paralleled changes in p65, as assessed by supershift analysis (Figure 7B).
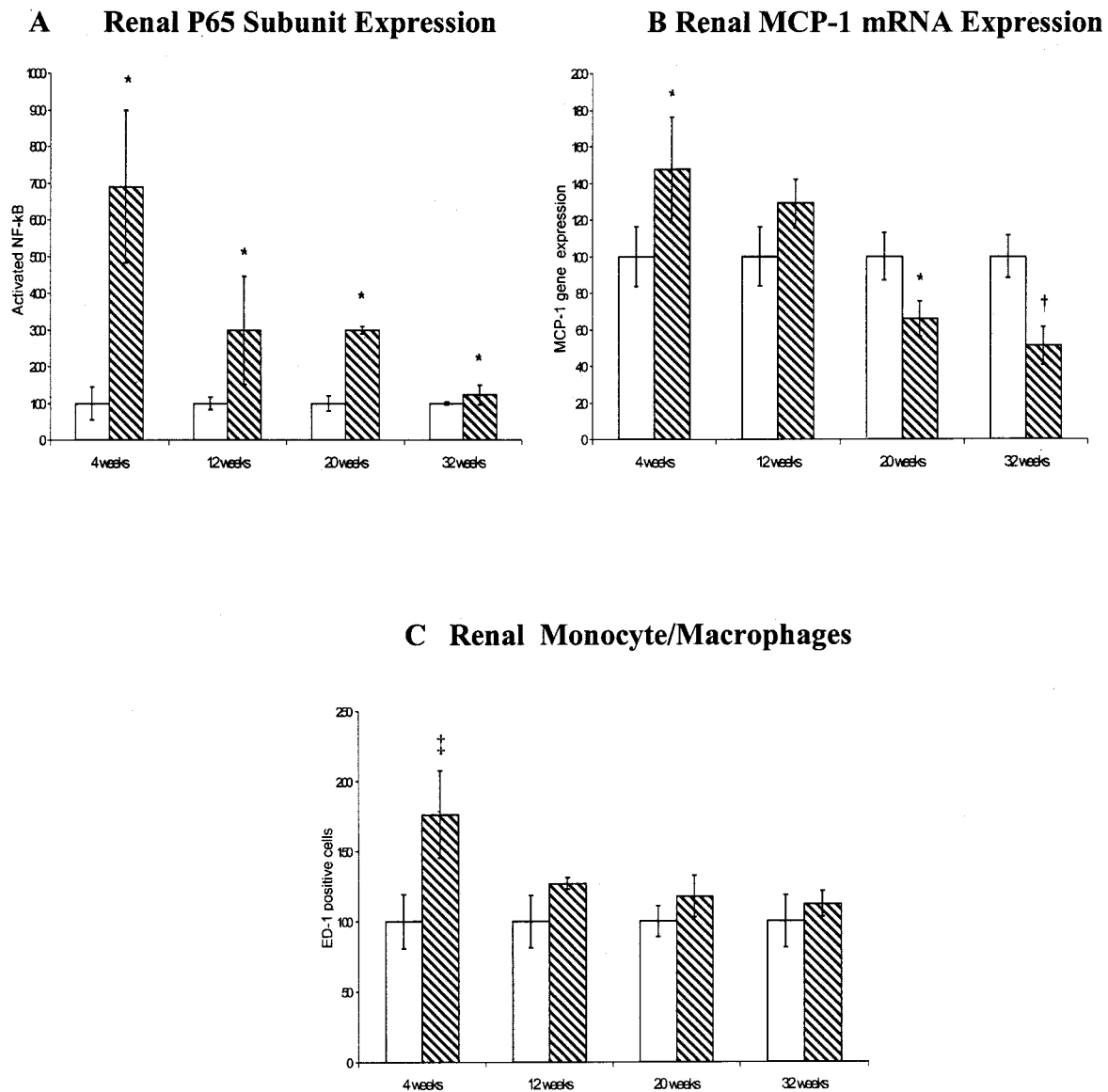
A   Renal P65 Subunit Expression

B Renal MCP-1 mRNA Expression

C   Renal Monocyte/Macrophages

Figure 2. Time course quantitative analysis of p65 band by EMSA supershift (A), gene expression of monocyte chemoattractant protein-1 (MCP-1) by real time reverse transcription–PCR (RT-PCR; B), and renal ED-1 immunohistochemistry for monocytes and macrophages (C). □, controls; ▨ diabetic groups. Diabetes was expressed as percentage change compared with control for p65 expression. *$P < 0.05$, †$P < 0.005$, ‡$P = 0.06$ *versus* control group at the same time point.

ED-1 Immunohistochemistry. Increased ED-1–positive monocytes/macrophages in diabetic animals was prevented by valsartan and PDTC treatment but not by PD123319 treatment (Figure 6C). These changes in ED-1 immunostaining paralleled changes in MCP-1 gene expression (Figure 6B) and p65 subunit, as assessed by supershift assay (Figure 6A).

Discussion

In the present study, temporal changes were identified in the expression of NF-κB and the p50 and p65 subunits in the renal cortex over the duration of diabetes. Total activated NF-κB as detected by EMSA correlated with changes in the p50 subunit. The proportion of the p65 subunit, however, was greater in diabetic animals at all time points when compared with control

animals but was maximally expressed at 4 wk of diabetes. These diabetes-induced increases in the activation of the p65 subunit of NF-κB were associated with an increase in the chemotactic factor MCP-1 as well as infiltration of macrophages. In addition, there was a modest increase in tubulointerstitial area seen at this time point with diabetes. These pathologic changes were attenuated by blockade of the RAS with valsartan and, importantly, the NF-κB inhibitor PDTC. PD123319 had modest effects on NF-κB expression. The inhibitory subunit of NF-κB, IκBα was significantly increased by week 12 of diabetes but was reduced significantly by 32 wk.

There is increasing evidence that inflammatory cells and cytokines contribute to diabetic nephropathy (3), and it has been identified that specific activation of the p65 subunit may
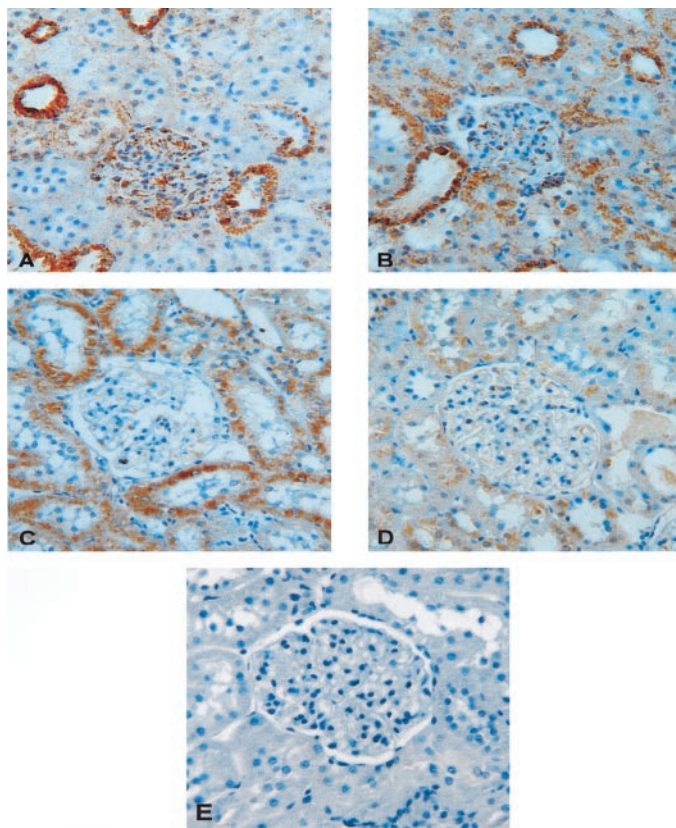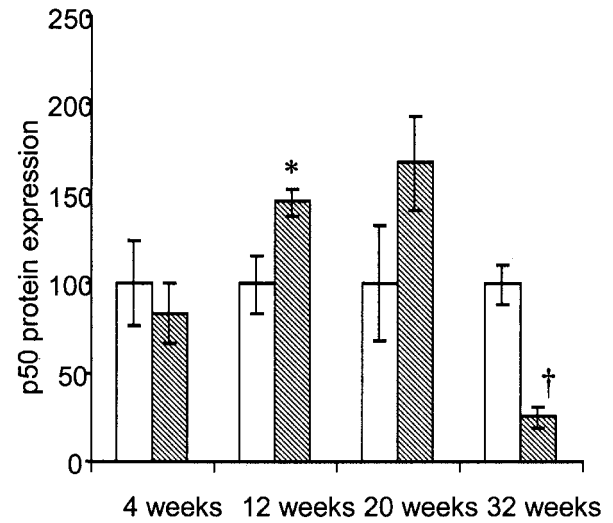
A   Renal P50 Subunit Expression

Figure 3. Representative photomicrographs of renal p50 immuno-staining in 4-wk control (A), 4-wk diabetic (B), 32-wk control (C), and 32-wk diabetic animals (D). (E) Negative control section with primary antibody omitted. Magnification, ×200.

be an important mediator of these events. Not only was p65 activation confirmed by EMSA, but also immunohistochemical studies at the 4-wk time point revealed nuclear translocation of the p65 subunit. Activation of this nuclear transcription factor subunit leads to production of chemokines, proinflammatory cytokines, and adhesion molecules. In particular, the chemo-kine MCP-1 is considered to be specifically activated by NF-κB (29), especially in the presence of high glucose (19). The present study demonstrated that MCP-1 expression corre-lated with p65 activation. There were parallel changes in p65 and MCP-1 expression, with the greatest increase in p65 and MCP-1 in diabetic animals occurring at 4 wk. The correlation between MCP-1 and p65 demonstrated *in vivo* in this study is consistent with previously reported *in vitro* findings by Ueda *et al.* (29). Total NF-κB activation and specific activation of the p50 subunit did not correlate with MCP-1 gene expression in diabetic animals. P50 activation was maximal at week 12, when MCP-1 gene expression had decreased. These findings are consistent with the view that the p50 subunit exists as a homodimer without an ability to cause transactivation of target genes, whereas the p65 subunit contains a transactivating do-main and therefore can activate transcription of target genes such as MCP-1 (1).

The temporal fluctuations in NF-κB in the diabetic context are occurring over weeks in this study and are in contrast to
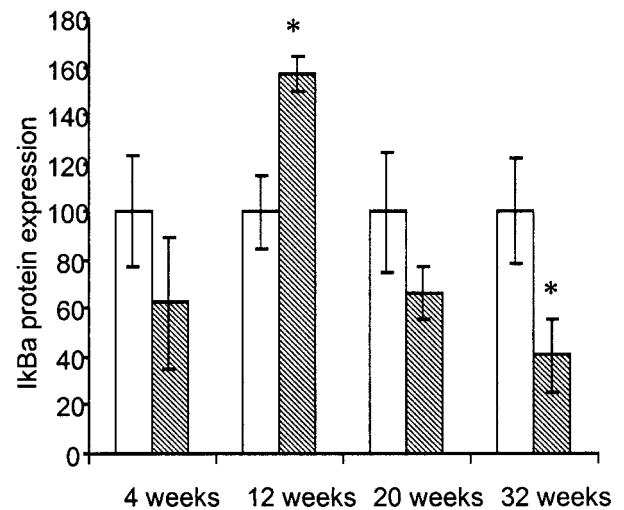
B   Renal IκB-α Expression

Figure 4. Morphologic quantification of renal immunostaining for the p50 subunit of NF-κB (A) and the native inhibitor of NF-κB, IκBα (B). □controls; ▨, diabetic rats. Diabetes expressed as percentage change compared with controls at the same time point. *$P < 0.05$, †$P < 0.001$ *versus* control of same time point.

those that would be predicted if the changes in NF-κB were part of an acute stress response. The response to acute stimuli, which has been studied more extensively in relation to NF-κB, has been shown to result in rapid phosphorylation of the inhibitory subunit IκBα, which detaches from the nuclear localization sequence to activate NF-κB (30), terminating within hours with the resynthesis and binding of IκBα. Thus,
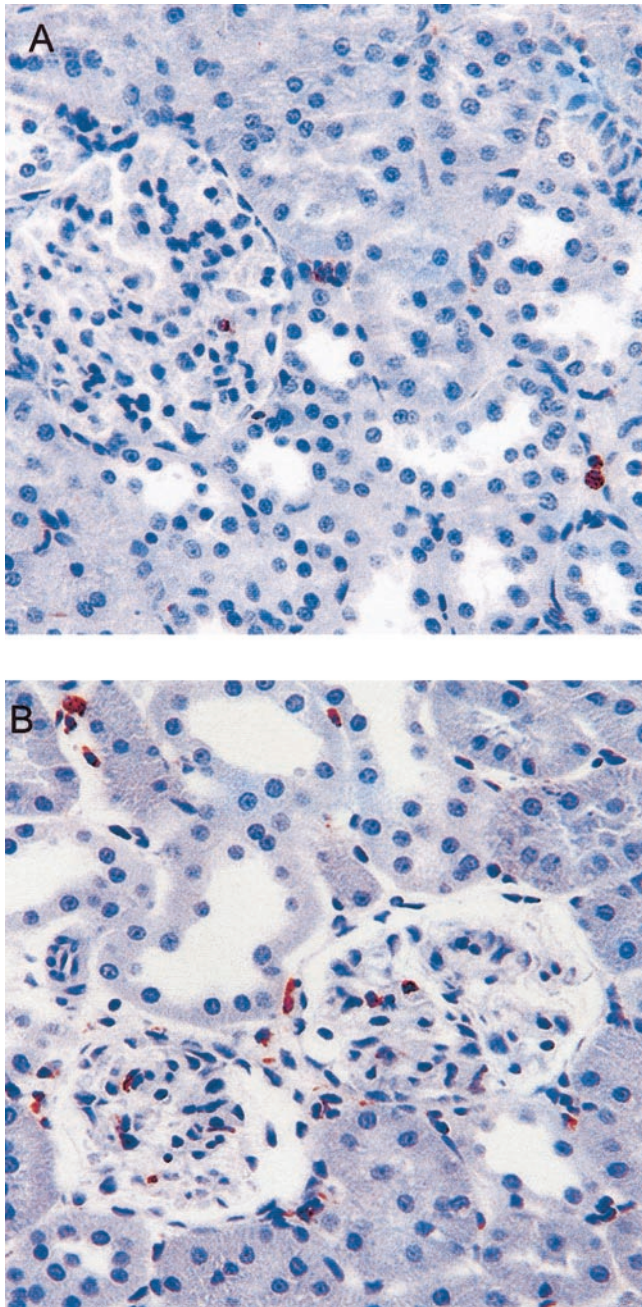
Figure 5. Representative photomicrographs of renal ED-1 immunostaining at week 4 in control (A) and diabetic rats (B). Magnification, ×400.

Table 2. Metabolic parameters in protocol 2: Treatment with inhibitors of RAS or NF-κB activation[a]

Group	n	Glucose (mmol/L)	Body Weight (g; Mean ± SD)	Kidney Weight (g)	Urine Volume (ml/24 h; Mean ± SD)	Blood Pressure (mm Hg)	AER[b] (mg/24 h)	Glomerulosclerotic Index	Tubulointerstitial Area (%)
Control	8	6.4 ± 0.2	410 ± 17	1.55 ± 0.04	16 ± 1	126 ± 3	0.28 ×/÷ 1.3	1.3 ± 0.3	2.1 ± 0.1
Diabetes	8	27.5 ± 0.5[c]	280 ± 9[c]	1.82 ± 0.06[d]	134 ± 8[c]	152 ± 5[c]	0.92 ×/÷ 1.1[c]	1.2 ± 0.3	3.0 ± 0.2[h]
D + Valsartan	8	30.6 ± 0.3[c]	290 ± 10[c]	1.56 ± 0.07[e]	157 ± 9[c]	137 ± 3[e]	0.75 ×/÷ 1.1[d]	0.9 ± 0.2[e,h]	1.6 ± 0.2[e,f]
D + PD123319	8	29.1 ± 0.7[c]	270 ± 9[c]	1.72 ± 0.09[f]	135 ± 14[c]	140 ± 3[f,g]	1.09 ×/÷ 1.1[c]	1.5 ± 0.2	2.7 ± 0.1[f]
D + PDTC	8	30.4 ± 1.3[c]	278 ± 9[c]	1.57 ± 0.06[e]	199 ± 11[c,e]	124 ± 4[e]	1.16 ×/÷ 1.1[c]	1.1 ± 0.1	2.1 ± 0.2[e]

[a] Data are shown as mean ± SEM. PDTC, pyrrolidone dithiocarbamate.
[b] Shown as geometric mean ×/÷ tolerance factor.
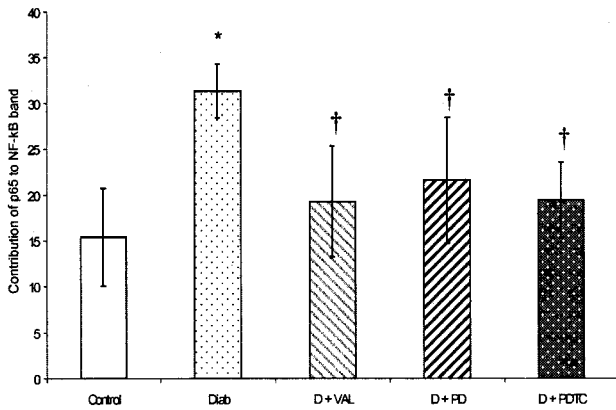[c] $P < 0.0001$ *versus* control.
[d] $P < 0.005$ *versus* control.
[e] $P < 0.01$ *versus* diabetes.
[f] $P < 0.05$ *versus* control.
[g] $P < 0.05$ *versus* diabetes.
[h] $P < 0.02$ *versus* control.

there is tightly controlled feedback inhibition occurring with acute stimuli to prevent persistent NF-κB activation (31). Our data demonstrated that IκBα levels correlate with activated NF-κB, and this is consistent with the fact that translocation of NF-κB to the nucleus causes upregulation of IκBα gene transcription. However, more recently, studies have suggested that this autoregulatory mechanism can be overcome in disease states to produce more prolonged activation of NF-κB (19). It is likely that such a mechanism is operative in a more chronic context such as is seen in the present renal diabetic study. One

A Renal P65 subunit Expression   B Renal MCP-1 Gene Expression
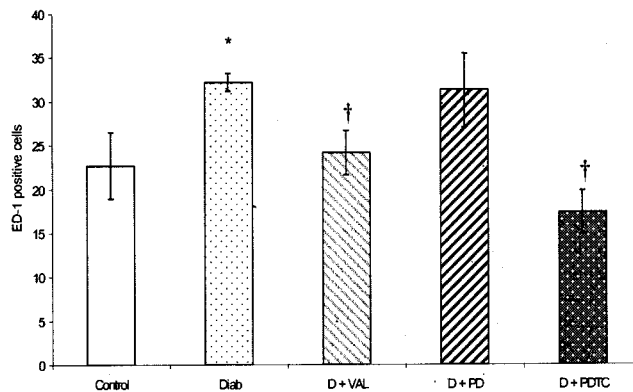
C Renal Monocytes/Macrophages

Figure 6. Protocol 2: (A) Quantification of p65 subunit by EMSA supershift. (B) Renal MCP-1 gene expression by real-time RT-PCR. (C) Renal ED-1 immunostaining for monocytes and macrophages. Data from EMSA for p65 are expressed as percentage contribution to total activated NF-κB band. D+VAL, diabetes + valsartan; D+PD, diabetes + PD123319; D+PDTC, diabetes + pyrrolidine dithiocarbamate. *$P < 0.05$ *versus* control; †$P < 0.05$ *versus* diabetes.

could speculate that the increases in both the expression of IκBα and of the nontransactivating subunit of NF-κB, p50, were an attempt to return the balance of renal gene expression toward control levels. This is supported by the reduction with diabetes at week 32 in each of these "protective" regulatory subunits, where the greatest degree of renal injury, as assessed by increases in tubulointerstitial area and glomerulosclerosis, in the context of increased albuminuria is seen. Indeed, this suggests that it may be the balance between "protective" IκBα and the pathogenic p65 subunit that is the most important determinant of renal damage. It is of interest that most rat

models of diabetes do not develop advanced renal disease or exhibit significant decline in renal function. It is possible that these "adaptive" changes including reduced NF-κB activation prevent ongoing severe and progressive renal injury (14,19,23). Diabetic animals had a trend toward increased renal monocyte/macrophage accumulation as assessed by ED-1 immunohistochemistry at all time points, particularly at 4 wk. Renal ED-1 immunostaining correlated with both MCP-1 gene expression and p65 activation, consistent with the previously reported associations between these pathways in the diabetic kidney (19,32). This link between NF-κB, MCP-1, and mac-

A   Total Renal Nf-κB – Protocol 2
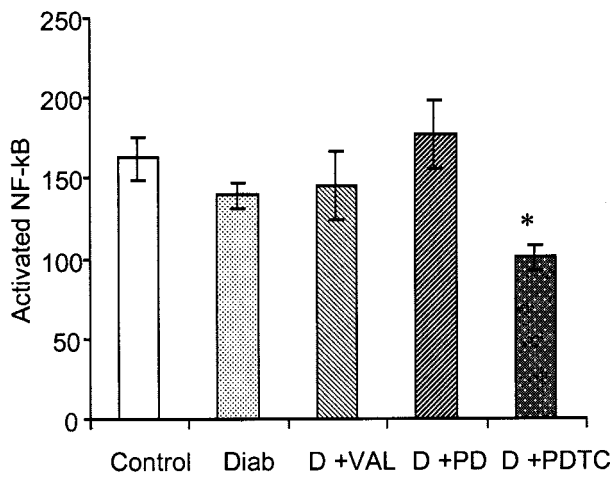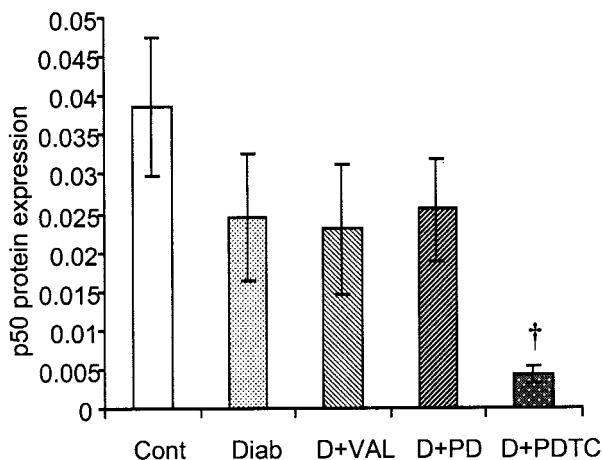

B   Renal P50 Expression – Protocol 2

Figure 7. Protocol 2: 4-wk treatment with renin angiotensin system (RAS) or NF-κB inhibitors. (A) Quantification of total renal activated NF-κB by EMSA. Density expressed as percentage of external control. (B) Morphometric quantification of p50 immunostaining . *$P < 0.01$ *versus* diabetes and $P < 0.05$ *versus* control. D+VAL, diabetes + valsartan; D+PD, diabetes + PD123319; D+PDTC, diabetes + pyrrolidine dithiocarbamate. †$P = 0.08$ *versus* diabetes and $P < 0.01$ *versus* control.

Figure 8. (A) Immunohistochemical staining for the activated p65 subunit of NF-κB in 4-wk control kidney and in 4-wk diabetic kidney (B). Arrows demonstrate cellular examples in which translocation of the activated p65 subunit of NF-κB from cytosol to nucleus has occurred. Magnification, ×400.

molecule-1, whose expression is NF-κB dependent (33). Consistent with our data, Young *et al.* (34) found glomerular macrophage infiltration beginning at 3 d and peaking at 30 d in diabetic rats. It is interesting that other groups have shown that infiltrating peripheral blood mononuclear cells themselves may contribute to the level of NF-κB activation (35), which is consistent with the correlation between infiltrating cells and active p65 subunits in the present study.

Activation of the NF-κB subunits p50 and p65 activation were localized predominately within the i tubules, although significant expression was also seen in glomeruli. The predominance of tubular expression is consistent with studies indicating that NF-κB–dependent proteins such as MCP-1 and the prosclerotic TGF-β1 and CTGF are produced by proximal tubules as assessed in both *in vitro* and *in vivo* approaches (36–40). The tubules account for the majority of the renal cortical mass, and tubulointerstitial injury therefore is an important feature of diabetic nephropathy (41). Indeed, an increase in tubulointerstitial area is the number one predictor of progressive renal disease. The present study showed significant tubulointerstitial expansion, which increased in a time-dependent manner in the diabetic animals. Nevertheless, it remains to be determined whether the interventions to reduce NF-κB will ultimately lead to long-term beneficial effects on renal structure and function. Blockade of the RAS has early effects that ultimately lead to long-term preservation of renal function (20,36–41). Indeed, the findings of the present study, in which interruption of the RAS influenced NF-κB activation, could partly explain some of the renoprotective effects observed with agents such as the AT1 receptor antagonist valsartan. The extent of glomerulosclerosis seen in the present study was less marked than tubulointerstitial changes.

Glomerular injury in this model seemed to be more clearly evident after the onset of tubulointerstitial changes. In general, glomerulosclerosis is detected in experimental diabetes after the development of macroalbuminuria, which occurs after at least 12 wk in this model (42). The issue of the relative involvement and importance of the glomerulus *versus* the renal tubule in the progression of diabetic nephropathy remains unresolved, although most investigators would agree that both renal compartments play a pivotal role (41).

rophage infiltration is consistent with the transcription of the chemokine MCP-1 being facilitated by the activation and translocation of the p65 subunit of NF-κB, which would contribute to early recruitment of macrophages in the diabetic kidney. It is likely that other factors are also involved, with hyperglycemia *per se* having been reported to induce another protein involved in macrophage recruitment, intracellular adhesion
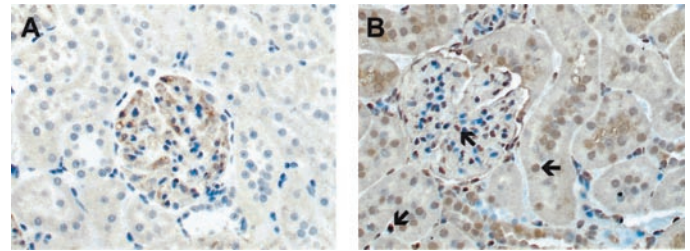
As the degree of p65 subunit activation was greatest at week 4 in the initial experiment, we proceeded to study the effects of inhibition of the RAS as compared with NF-κB blockade at this time point (protocol 2). Increased MCP-1 gene expression in diabetic animals was attenuated by treatment with AT1 antagonism and with the AT2 receptor antagonist to a lesser degree. Treatment with the AT1 receptor antagonist also reduced the macrophage infiltration, although this effect was not seen with the AT2 antagonist. In the present study, the AT1 receptor was shown to be important in mediating inflammatory effects and cellular infiltration as has been described previously, albeit in a nondiabetic context (43). These molecular and cellular effects of the AT1 receptor antagonist translated to a decrease in tubulointerstitial area. By contrast, the AT2 receptor blocker did not significantly influence macrophage infiltration and therefore tubulointerstitial area in this model.

NF-κB blockade by PDTC resulted in a similar degree of inhibition of MCP-1 gene expression and subsequent macrophage infiltration as observed with the AT1 antagonist. This is consistent with NF-κB being a major pathway by which AII mediates inflammatory responses in this model, primarily via the AT1 receptor as suggested within this model. Such a possibility has previously been shown in vitro, where NF-κB activation by AII increased expression of MCP-1 in cultured rat mesangial and mononuclear cells (10,11). Blockade of the RAS has also been shown specifically to reduce MCP-1 expression in short-term experimental diabetes (32). Although NF-κB was not implicated in that study, it is interesting to note that the major increases found were MCP-1 and IL-1β, which both are postulated to be regulated by NF-κB. A role for both AT1 and AT2 receptors in AII-mediated activation of NF-κB has been demonstrated by Wolf et al. in vitro (44) and by Ruiz-Ortega et al. (10,45) in vivo. Our data are consistent with these findings but suggest a more dominant role for the AT1 over the AT2 receptor subtype, as both PDTC and AT1 receptor blockade showed greater inhibition of MCP-1 expression and macrophage infiltration than AT2 receptor blockade. Further evidence to suggest a more dominant role for the AT1 rather than the AT2 receptor subtype in mediating various markers of renal injury can be identified in the present study with a more powerful effect of valsartan versus PD123319 in attenuating diabetes-associated renal hypertrophy and tubulointerstitial expansion. Although there is increasing evidence that the AT2 receptor may play a role in chronic renal disease, these data support the hypothesis that the AT1 receptor plays a more significant role (46). In the present study, 4 wk of diabetes was associated with changes in the p65 subunit, which paralleled the changes seen in MCP-1 gene expression and macrophage infiltration. Blockade of AT1, AT2, or NF-κB reduced p65 activation in diabetic animals, although to different degrees as discussed above. This suggests that not only is p65 an important correlate of downstream markers of inflammation, but it also seems to be the major subunit involved in the signaling pathway of AII, which ultimately leads to the inflammatory response.

This study has provided in vivo evidence that there are temporal changes in NF-κB with the evolution of experimental diabetic nephropathy. NF-κB, in particular the p65

subunit, seems to be an important mediator of the effects of AII predominately via the AT1 receptor but also the AT2 receptor subtype, resulting in an increase in MCP-1 expression and macrophage infiltration in the early stages of experimental diabetes. The similarity in the effects observed with the AT1 receptor antagonist and the NF-κB inhibitor PDTC provides additional evidence linking activation of NF-κB by RAS to diabetes-associated renal injury. In the context of the known proinflammatory effects of AII, it is postulated that the renoprotection conferred by AII receptor antagonism is at least partly related to the inhibition of NF-κB dependent pathways.

References

1. Auwardt RB, Mudge SJ, Power DA: Transcription factor NF-kappa B in glomerulonephritis. *Nephrology* 5: 71–82, 2000
2. Guijarro C, Egido J: Transcription factor-kappa B (NF-kappa B) and renal disease. *Kidney Int* 59: 415–424, 2001
3. Chuang LY, Guh JY: Extracellular signals and intracellular pathways in diabetic nephropathy. *Nephrology* 6: 165–172, 2001
4. Cooper ME: Interaction of metabolic and haemodynamic factors in mediating experimental diabetic nephropathy. *Diabetologia* 44: 1957–1972, 2001
5. Pieper GM, Riaz-ul-Haq: Activation of nuclear factor-kappa-b in cultured endothelial cells by increased glucose concentration—Prevention by calphostin C. *J Cardiovasc Pharmacol* 30: 528–532, 1997
6. Yerneni KKV, Bai W, Khan BV, Medford RM, Natarajan R: Hyperglycemia-induced activation of nuclear transcription factor kappa B in vascular smooth muscle cells. *Diabetes* 48: 855–864, 1999
7. Lewis EJ, Hunsicker LG, Bain RP, Rhode RD: The effect of angiotensin converting enzyme inhibition on diabetic nephropathy. *N Engl J Med* 329: 1456–1462, 1993
8. Wolf G: Molecular mechanisms of angiotensin II in the kidney: Emerging role in the progression of renal disease: Beyond haemodynamics. *Nephrol Dial Transplant* 13: 1131–1142, 1998
9. Suzuki Y, Ruiz-Ortega M, Egido J: Angiotensin II: A double-edged sword in inflammation. *J Nephrol* 13[Suppl 3]: S101–S110, 2000
10. Ruiz-Ortega M, Lorenzo O, Ruperez M, Konig S, Wittig B, Egido J: Angiotensin II activates nuclear transcription factor kappa B through AT(1) and AT(2) in vascular smooth muscle cells—Molecular mechanisms. *Circ Res* 86: 1266–1272, 2000
11. Ruiz-Ortega M, Bustos C, Hernandez-Presa MA: Angiotensin II participates in mononuclear cell recruitment in experimental immune complex nephritis through nuclear factor-kB activation and monocyte chemoattractant protein-1 synthesis. *J Immunol* 161: 430–439, 1998

12. Gomez-Garre D, Largo R, Tejera N: Activation of NF-kB in tubular epithelial cells of rats with intense proteinuria. Role of angiotensin II and endothelin-1. *Hypertension* 37: 1171–1178, 2001

13. Morrissey JJ, Klahr S: Enalapril decreases nuclear factor kappa-b activation in the kidney with ureteral obstruction. *Kidney Int* 52: 926–933, 1997

14. Banba N, Nakamura T, Matsumura M, Kuroda H, Hattori Y, Kasai K: Possible relationship of monocyte chemoattractant protein-1 with diabetic nephropathy. *Kidney Int* 58: 684–690, 2000

15. Martin T, Cardarelli PM, Parry GCN, Felts KA, Cobb RR: Cytokine induction of monocyte chemoattractant protein-1 gene expression in human endothelial cells depends on the cooperative action of NF-kappa-B and Ap-1. *Eur J Immunol* 27: 1091–1097, 1997

16. Landry DB, Couper LL, Bryant SR, Lindner V: Activation of the NF-kappa-B and I-kappa B system in smooth muscle cells after rat arterial injury—Induction of vascular cell adhesion molecule-1 and monocyte chemoattractant protein-1. *Am J Pathol* 151: 1085–1095, 1997

17. Wang YP, Rangan GK, Tay YC, Wang Y, Harris DCH: Induction of monocyte chemoattractant protein-1 by albumin is mediated by nuclear factor kappa B in proximal tubule cells. *J Am Soc Nephrol* 10: 1204–1213, 1999

18. Rovin BH, Dickerson JA, Tan LC, Hebert CA: Activation of nuclear factor-kappa-B correlates with Mcp-1 expression by human mesangial cells. *Kidney Int* 48: 1263–1271, 1995

19. Bierhaus A, Schiekofer S, Schwaninger M, Andrassy M, Humpert PM, Chen J, Hong M, Luther T, Henle T, Kloting I, Morcos M, Hofmann M, Tritschler H, Weigle B, Kasper M, Smith M, Perry G, Schmidt AM, Stern DM, Haring HU, Schleicher E, Nawroth PP: Diabetes-associated sustained activation of the transcription factor nuclear factor-kappa B. *Diabetes* 50: 2792–2808, 2001

20. Cao Z, Cooper ME, Wu LL, Cox AJ, Jandeleit-Dahm K, Kelly DJ, Gilbert RE: Blockade of the renin-angiotensin and endothelin systems on progressive renal injury. *Hypertension* 36: 561–568, 2000

21. Rangan GK, Wang YP, Tay YC, Harris DCH: Inhibition of nuclear factor-kappa B activation reduces cortical tubulointerstitial injury in proteinuric rats. *Kidney Int* 56: 118–134, 1999

22. Cefalu WT, Wang ZQ, Bell-Farrow A, Kiger FD, Izlar C: Glycohemoglobin measured by automated affinity HPLC correlates with both short-term and long-term antecedent glycemia. *Clin Chem* 40: 1317–1321, 1994

23. Soulis T, Cooper ME, Vranes D, Bucala R, Jerums G: Effects of aminoguanidine in preventing experimental diabetic nephropathy are related to the duration of treatment. *Kidney Int* 50: 627–634, 1996

24. Buñag RD: Validation in awake rat of a tail-cuff method for measurement of systolic blood pressure. *J Appl Physiol* 34: 279–282, 1973

25. Forbes JM, Cooper ME, Thallas V, Burns WC, Thomas MC, Brammar GC, Lee F, Grant SL, Burrell LA, Jerums G, Osicka TM: Reduction of the accumulation of advanced glycation end products by ACE inhibition in experimental diabetic nephropathy. *Diabetes* 51: 3274–3282, 2002

26. Smith PK, Krohn RI, Hermanson GT, Mallia AK, Gartner FH, Provenzano MD, Fujimoto EK, Goeke NM, Olson BJ, Klenk DC: Measurement of protein using bicinchoninic acid. *Anal Biochem* 150: 76–85, 1985

27. Youssef S, Nguyen DT, Soulis T, Panagiotopoulos S, Jerums G, Cooper ME: Effect of diabetes and aminoguanidine therapy on renal advanced glycation end-product binding. *Kidney Int* 55: 907–916, 1999

28. Bonnet F, Cooper ME, Kawachi H, Allen TJ, Boner G, Cao ZM: Irbesartan normalises the deficiency in glomerular nephrin expression in a model of diabetes and hypertension. *Diabetologia* 44: 874–877, 2001

29. Ueda A, Ishigatsubo Y, Okubo T, Yoshimura T: Transcriptional regulation of the human monocyte chemoattractant protein-1 gene—Cooperation of two NF-kappa-B sites and NF-kappa-B/Rel subunit specificity. *J Biol Chem* 272: 31092–31099, 1997

30. Baldwin AS: The transcription factor NF-kappa B and human disease. *J Clin Invest* 107: 3–6, 2001

31. Tran K, Merika M, Thanos D: Distinct functional properties of I-kappa-B-alpha and I-kappa-B-beta. *Mol Cell Biol* 17: 5386–5399, 1997

32. Kato S, Luyckx VA, Ots M, Lee KW, Ziai F, Troy JL, Brenner BM, Mackenzie HS: Renin-angiotensin blockade lowers MCP-1 expression in diabetic rats. *Kidney Int* 56: 1037–1048, 1999

33. Park CW, Kim JH, Lee JW, Kim YS, Ahn HJ, Shin YS, Kim SY, Choi EJ, Chang YS, Bang BK: High glucose-induced intercellular adhesion molecule-1 (ICAM-1) expression through an osmotic effect in rat mesangial cells is PKC-NF-kappa B-dependent. *Diabetologia* 43: 1544–1553, 2000

34. Young BA, Johnson RJ, Alpers CE, Eng E, Gordon K, Floege J, Couser WG: Cellular events in the evolution of experimental diabetic nephropathy. *Kidney Int* 47: 935–944, 1995

35. Hofmann MA, Schiekofer S, Isermann B, Kanitz M, Henkels M, Joswig M, Treusch A, Morcos M, Weiss T, Borcea V, Khalek A, Amiral J, Tritschler H, Ritz E, Wahl P, Ziegler R, Bierhaus A, Nawroth PP: Peripheral blood mononuclear cells isolated from patients with diabetic nephropathy show increased activation of the oxidative-stress sensitive transcription factor NF-kappa B. *Diabetologia* 42: 222–232, 1999

36. Oldfield MD, Bach LA, Forbes JM, Nikolic-Paterson D, McRobert A, Thallas V, Atkins RC, Osicka T, Jerums G, Cooper ME: Advanced glycation end products cause epithelial-myofibroblast transdifferentiation via the receptor for advanced glycation end products (RAGE). *J Clin Invest* 108: 1853–1863, 2001

37. Kelly DJ, Gilbert RE, Cox AJ, Soulis T, Jerums G, Cooper ME: Aminoguanidine ameliorates overexpression of prosclerotic growth factors and collagen deposition in experimental diabetic nephropathy. *J Am Soc Nephrol* 12: 2098–2107, 2001

38. Twigg SM, Cao Z, Clennan S, Burns WC, Brammar G, Forbes JM, Cooper ME: Renal connective tissue growth factor induction in experimental diabetes is prevented by aminoguanidine. *Endocrinology* 143: 4907–4915, 2002

39. Harris DC, Wang Y, Campbell D: Regulation of tubular cell MCP-1 production by intracellular ions: A role for sodium and calcium. *Exp Nephrol* 9: 205–213, 2001

40. Mezzano SA, Barria M, Droguett MA, Burgos ME, Ardiles LG, Flores C, Egido J: Tubular NF-kappa B and AP-1 activation in human proteinuric renal disease. *Kidney Int* 60: 1366–1377, 2001

41. Gilbert RE, Cooper ME: The tubulointerstitium in progressive diabetic kidney disease: More than an aftermath of glomerular injury? *Kidney Int* 56: 1627–1637, 1999

42. Gilbert RE, Cox A, Wu LL, Allen TJ, Hulthen UL, Jerums G, Cooper ME: Expression of transforming growth factor-beta-1 and type IV collagen in the renal tubulointerstitium in experimental diabetes—Effects of ACE inhibition. *Diabetes* 47: 414–422, 1998

43. Wolf G, Ziyadeh FN, Thais F, Tomaszewiski J, Caron RJ, Wenzel U, Zahner G, Helmchen U, Stahl RAK: Angiotensin II stimulates expression of the chemokine RANTES in rat glomerular endothelial cells. Role of the angiotensin type 2 receptor. *J Clin Invest* 100: 1047–1058, 1997

44. Wolf G, Wenzel U, Burns KD, Harris RC, Stahl RAK, Thais F: Angiotensin II activates nuclear transcription factor-κB through AT_1 and AT_2 receptors. *Kidney Int* 61: 1986–1995, 2002

45. Ruiz-Ortega M, Lorenzo B, Ruperez M, Blanco J, Egido J: Systemic infusion of angiotensin II into normal rats activates nuclear factor-kappa B and AP-1 in the kidney—Role of AT(1) and AT(2) receptors. *Am J Pathol* 158: 1743–1756, 2001

46. Cao Z, Bonnet F, Candido R, Nesteroff SP, Burns WC, Kawachi H, Shimizu F, Carey RM, De Gasparo M, Cooper ME: Angiotensin type 2 receptor antagonism confers renal protection in a rat model of progressive renal injury. *J Am Soc Nephrol* 13: 1773–1787, 2002